

# Demonstration of Encoding and Decoding 2-D Wavelength-Time Bipolar Codes for OCDMA Systems With Differential Detection

Rhys Adams, *Student Member, IEEE*, Julien Faucher, *Student Member, IEEE*, Luay Thomas, David V. Plant, *Senior Member, IEEE*, and Lawrence R. Chen, *Member, IEEE*

**Abstract**—We provide the first demonstration of encoding–decoding two-dimensional wavelength-time bipolar codes for optical code-division multiple access systems with differential detection, including a verification of multiaccess interference rejection. We implement the all-optical encoders and decoders using commercially available wavelength-division-multiplexing components.

**Index Terms**—Balanced detection, bipolar signaling, optical code-division multiple-access (OCDMA), optical fiber communications.

## I. INTRODUCTION

OPTICAL code-division multiple-access (OCDMA) is attractive for networks carrying bursty, asynchronous traffic. Multidimensional coding approaches, for example wavelength-time ( $\lambda - t$ ), have been investigated as a means for providing greater flexibility in code design, increasing the number of simultaneous users, and increasing potential data throughput. In particular, two-dimensional wavelength-time (2-D  $\lambda - t$ ) OCDMA has attracted attention since it can exploit standard wavelength-division-multiplexing (WDM) components, such as array waveguide gratings (AWGs), optical power splitters–combiners, and fiber delay lines. However, the use of on–off keying and direct detection, i.e., unipolar codes, limits system bit-error-rate (BER) performance. On the other hand, it is well known that differential detection and bipolar coding can be used to reduce, or even eliminate, multiaccess interference (MAI), thereby improving system performance [1]–[5]. Recently, there have been several investigations on designing and theoretically analyzing the system performance of 2-D  $\lambda - t$  bipolar codes and indeed, simulations clearly show the superiority of the approach: A larger number of simultaneous users can operate at a lower BER compared to the unipolar case.

Although different encoder–decoder structures have been proposed to implement 2-D  $\lambda - t$  bipolar codes [1], [3]–[5], to date there have been no experimental demonstrations. In

Manuscript received February 24, 2005; revised June 20, 2005. This work was supported in part by FQRNT, in part by McGill University (Tomlinson Fellowship), in part by Anritsu Electronics Ltd., in part by CIPI, and in part by the Agile All-Photonic Networks (AAPN) Research Program.

The authors are with the Photonic Systems Group, Department of Electrical and Computer Engineering, McGill University, Montréal, QC H3A 2A7, Canada (e-mail: adamsrhys@gmail.com; julienf@photonics.ece.mcgill.ca; lthomas@ece.mcgill.ca; plant@photonics.ece.mcgill.ca; chen@photonics.ece.mcgill.ca).

Digital Object Identifier 10.1109/LPT.2005.857246

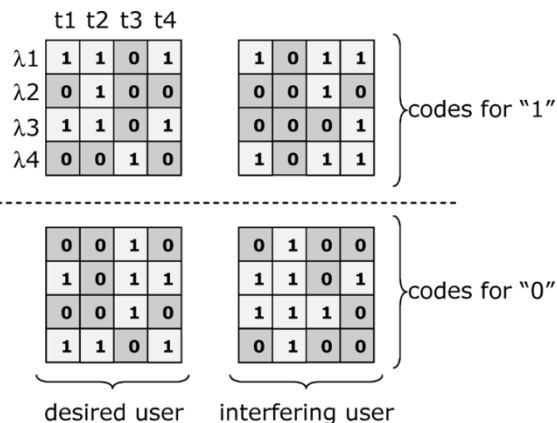


Fig. 1. Two BCDDs where  $m = n = 4$  and  $\kappa = 1$  used to demonstration encoding and decoding of 2-D  $\lambda - t$  bipolar codes.

this letter, we demonstrate for the first time the successful encoding and decoding of 2-D  $\lambda - t$  bipolar codes based on the balanced codes for differential detection (BCDD) [2], including a verification of MAI rejection using differential detection.

## II. EXPERIMENTAL SETUP AND RESULTS

Briefly, BCDDs are a family of high weight codes satisfying the following constraints: 1) the Hamming weight of each code is half of the code size; 2) the maximum autocorrelation side-lobe of the spreading codes for "1" and "0" (positive and negative codes) is at most  $\kappa$ ; and 3) the maximum cross correlation of each positive and negative code is also at most  $\kappa$  [2]. Moreover, for a given user, the codes for "1" and "0" are complementary (note that the encoded waveforms for "1" and "0" are positive signals). The codes are designed to exploit differential detection for suppressing MAI (averaged over a bit window), thereby resulting in improved performance [2].

In this proof-of-principle demonstration, we consider BCDDs with  $m = 4$  wavelengths,  $n = 4$  time chips, and  $\kappa = 1$ . This choice of code parameters results in only a modest number of users; however, as discussed in [2], the number of codes can be increased (up to  $m \times n$ ) by relaxing the cross correlation  $\kappa$ . We consider two users, one desired and one interfering, whose codes are illustrated in Fig. 1.

Fig. 2(a) shows a high-level schematic of the OCDMA network and our experimental setup for encoding and decoding the two BCDDs shown in Fig. 1; the system parameters are given in Table I. Unlike unipolar coding, a signal is transmitted even when

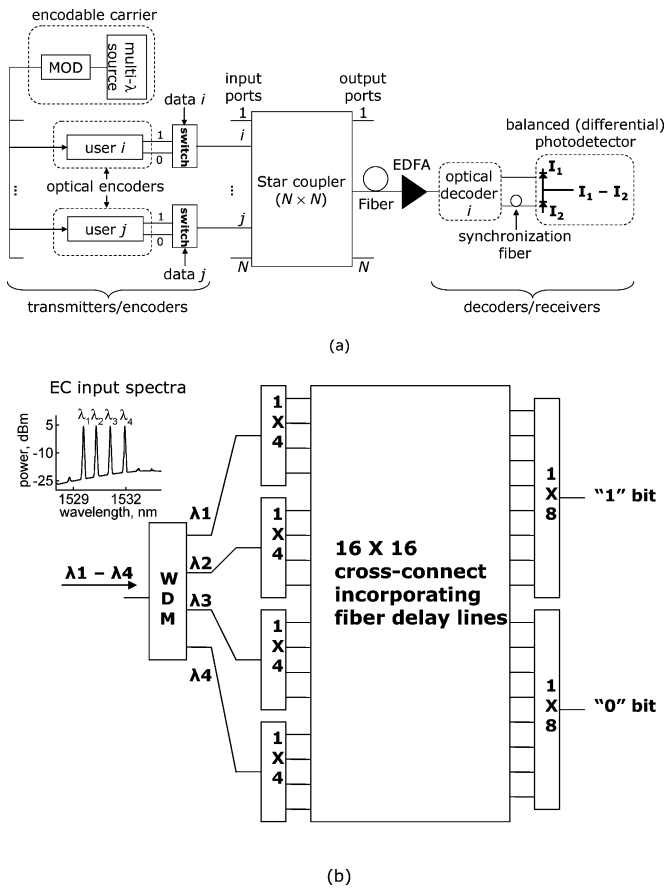


Fig. 2. (a) High-level schematic of network architecture and experimental setup. (b) Structure of the encoder-decoder.

TABLE I  
OCDMA SYSTEM DEMONSTRATION PARAMETERS

Parameter	Value
Wavelength range	1529.57, 1530.30, 1531.10, 1531.94 nm
Data rate	155.52 Mbps (OC-3)
Chip rate	622.08 Mbps (OC-12)
Balanced PD bandwidth	800 MHz

a user sends a “0”. A positive-peaked return-to-zero (RZ) pulse is used to represent the “1” or “0” data bits at the transmitter; the difference is that a “1” would result in a positive signal at the receiver whereas a “0” would result in a negative signal. This is possible using a balanced (differential) photodetector (PD).

We assume a broadcast-and-select star topology and as in [6], to simplify component cost, we assume an OCDMA network in which a central office generates an encodable carrier (EC), which is an RZ pulse having a duration equal to the chip window ( $\approx 1.6$ -ns duration) at the four wavelengths. It is obtained by modulating the output from a multiwavelength source comprising four distributed feedback lasers (the duty cycle of the pulsewidth relative to the bit rate is  $1/n$  or here,  $1/4$ ). The peak power per wavelength in the EC is  $\approx 4.3$  dBm. Note that the EC represents either a “1” or a “0”.

Each user then encodes the EC optically, i.e., generates the BCDDs, using the encoder structure shown in Fig. 2(b). The encoder consists of an AWG for wavelength selection, power

splitters, fiber delay lines, and power combiners. It comprises two interconnected encoder structures nominally used to generate 2-D  $\lambda - t$  unipolar codes, one for each “1” and “0”. Since the BCDDs are designed to allow for multiple pulse per row (the same wavelength can occupy multiple time chips) or multiple pulse per column (multiple wavelengths occupy the same time chip), the pulses at each of the  $m = 4$  wavelengths are divided (in power)  $n = 4$  times. A  $(m \times n) \times (m \times n) = 16 \times 16$  cross connect is then used to induce the appropriate delays and direct the delayed pulses at each wavelength to the appropriate output for an encoded “1” or “0”. The “1” and “0” output ports are temporally synchronized, i.e., the encoded “1” and “0” signals have a common temporal reference. They are connected by a fast optical switch driven by the corresponding data to be sent in order to select between the “1” and “0” output ports. The output of the switches from the different users are then connected to the star coupler for broadcasting. Note that the implementation of 2-D  $\lambda - t$  bipolar codes is significantly more complex than one-dimensional bipolar spectral codes since the signals need to be de-spread temporally before differential detection.

The decoder has the same architecture, except with complementary time delays with respect to the corresponding encoder. The decoder has two outputs: the top port for a “1” and the bottom port for a “0”. The two ports are connected to a commercial balanced PD with a bandwidth of 800 MHz (New Focus 1617). A length of fiber is used to synchronize the “1” and “0” output ports of the optical decoder for proper differential detection. We note that our proposed encoder-decoder structure can be used to implement other families of 2-D  $\lambda - t$  bipolar codes and is not limited to BCDDs.

The four wavelengths are set so as to minimize the effect of wavelength mismatch of the AWGs in the encoders and decoder. The time delays are obtained by splicing appropriate lengths of fiber, each carefully measured to within  $\pm 5\%$  of a time chip in order to minimize the effects of temporal mismatch in the encoder-decoder. The insertion loss of each encoder or decoder is  $\approx 21$  dB and includes the insertion loss of the AWG and losses from the splitters, combiners, and splices (the uniformity of the insertion losses is within 1 dB).

For matched filtering, i.e., a properly decoded signal, the autocorrelation peak for a “1” generates a positive output ( $I_1$ ) from the PD, whereas it generates a negative output ( $-I_2$ ) for a “0”. For an improperly matched user, the decoder output is always 0 in the middle of the cross correlation window (the total MAI integrates to 0 over the bit window).

In our experiment, we replace the fast optical switches shown in Fig. 2(a) with slow mechanical ones. The switches are not driven by the data so that at any given time, we can only encode (and, hence, decode) “1” or “0” bits. Moreover, for multiuser operation, both desired and interfering users transmit all “1” or “0”, though they do not have to transmit the same data bits. We emphasize that this limitation in our demonstration is only due to component availability and does not present any fundamental limitation.

The results of encoding a single “1” or “0” for the desired user are shown in Fig. 3(a). In this case, the encoded waveform was measured using an optical sampling module with a rise time of  $\approx 30$  ps. The temporal and spectral traces clearly match the

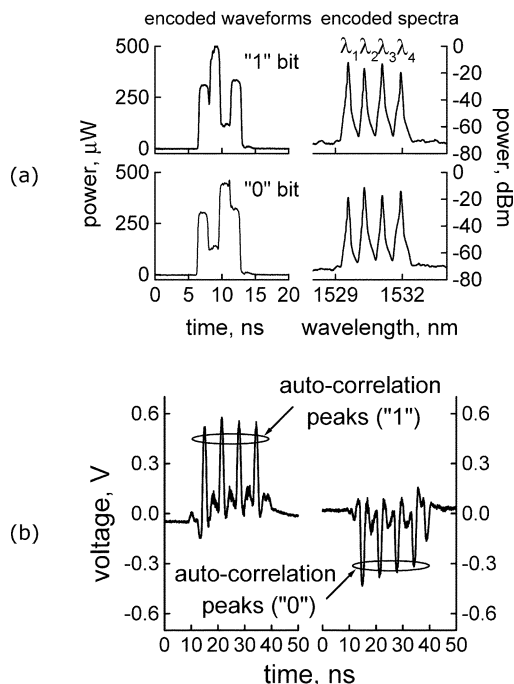


Fig. 3. (a) Encoded waveforms and spectra for "1" and "0" bits for desired user. (b) PD output when desired user transmits four consecutive "1" or "0" bits.

BCDD patterns illustrated in Fig. 1. For example, in the waveform of an encoded "1", the peak in the second time chip is largest since there are three wavelengths present ( $\lambda_1$ ,  $\lambda_2$ ,  $\lambda_3$ ), whereas the peak in the third time chip is smallest (only  $\lambda_4$  is present). Also, in terms of the spectral traces, the power at wavelengths  $\lambda_1$  and  $\lambda_3$  is approximately equal and greater than that at  $\lambda_2$  and  $\lambda_4$  ( $\lambda_1$  and  $\lambda_3$  have three active chips compared to only one for  $\lambda_2$  and  $\lambda_4$ ). The PD output when four consecutive "1" or "0" bits are transmitted is shown in Fig. 3(b). The principle positive and negative peaks correspond to the autocorrelation peaks for "1" and "0", respectively, and are clearly distinguishable. The sidelobes are expected, based on the code properties [2]. The measured temporal and spectral traces for the interfering user (not shown) also match the corresponding BCDD patterns in Fig. 1.

In Fig. 4(a), we show the PD output when the desired user transmits either a "1" or "0" while the interfering user transmits a "1". In this case, there is a temporal offset between the decoded signals of the desired and interfering user due to the use of a short (3 m) fiber patchcord between the two users and the star coupler (this was used to visually distinguish the cross correlation from the autocorrelation peak). The positive or negative autocorrelation peaks for the desired user are clearly distinguishable. In fact, the presence of the interfering user has negligible impact since it is largely suppressed by differential detection. This can be seen more clearly in Fig. 4(b) which compares the PD output when 1) the desired user transmits two consecutive "0" bits and the interfering user transmits two consecutive "1" bits and 2) only the desired user transmits two consecutive "0" bits (note that in this case, the autocorrelation and cross correlation signals overlap partially). The traces are practically indistinguishable. Similar results are obtained when the desired and interfering users transmit, respectively, "1" and "0", "1" and "1", or "0" and "0". Similar results are also obtained when we remove the short patchcord and increase the number of consec-

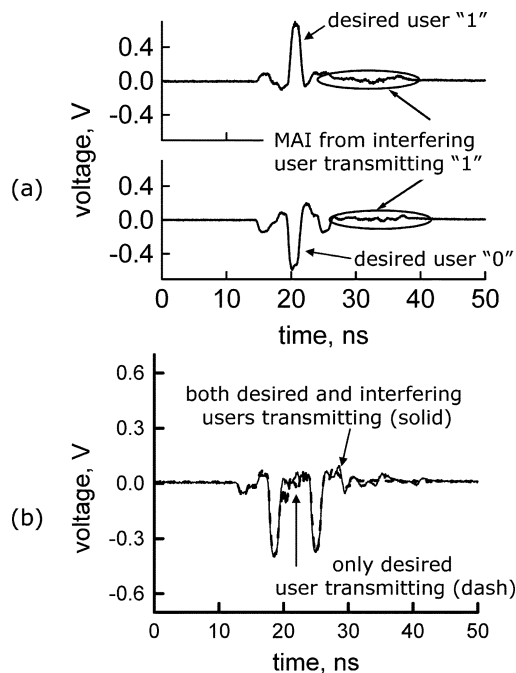


Fig. 4. PD output when (a) desired user transmits "1" or "0" while interfering user transmits "1" and (b) desired (interfering) user transmits two consecutive "0" ("1") bits.

utive transmitted bits from two to four. This shows that balanced detection is effective at minimizing MAI.

### III. SUMMARY

We provided the first experimental demonstration of successful encoding and decoding of 2-D  $\lambda - t$  bipolar codes, including a verification of MAI rejection using differential detection. We constructed the encoders–decoders using commercially available WDM components. These results show the viability and potential of 2-D  $\lambda - t$  bipolar codes for OCDMA systems.

### ACKNOWLEDGMENT

The authors thank R. M. H. Yim, J. Bajcsy, and N. Bélanger (McGill) for their contributions and ITF Optical Technologies for component characterization.

### REFERENCES

- [1] S. P. Wan and Y. Hu, "Two-dimensional optical CDMA differential system with prime/OOC codes," *IEEE Photon. Technol. Lett.*, vol. 13, no. 12, pp. 1373–1375, Dec. 2001.
- [2] R. M. H. Yim, J. Bajcsy, and L. R. Chen, "A new family of 2-D wavelength-time codes for optical CDMA with differential detection," *IEEE Photon. Technol. Lett.*, vol. 15, no. 1, pp. 165–167, Jan. 2003.
- [3] U. N. Griner and S. Arnon, "A novel bipolar wavelength-time coding scheme for optical CDMA systems," *IEEE Photon. Technol. Lett.*, vol. 16, no. 1, pp. 332–334, Jan. 2004.
- [4] H. Heo, S.-S. Min, Y. H. Won, B. K. Kim, and B. W. Kim, "A new family of 2-D wavelength-time spreading code for optical code-division multiple-access system with balanced detection," *IEEE Photon Technol. Lett.*, vol. 16, no. 9, pp. 2189–2191, Sep. 2004.
- [5] W. C. Kwong, G.-C. Yang, and C.-Y. Chang, "Wavelength-hopping time-spreading optical CDMA with bipolar codes," *J. Lightw. Technol.*, vol. 23, no. 1, pp. 260–267, Jan. 2005.
- [6] A. J. Mendez, R. M. Gagliardi, V. J. Hernandez, C. V. Bennett, and W. J. Lennon, "High-performance optical CDMA system based on 2-D optical orthogonal codes," *J. Lightw. Technol.*, vol. 22, no. 11, pp. 2409–2419, Nov. 2004.